



Article

Spatial and Temporal Variations of PM_{2.5} and Its Relation to Meteorological Factors in the Urban Area of Nanjing, China

Tao Chen ¹, Jun He ², Xiaowei Lu ³, Jiangfeng She ^{1,*} and Zhongqing Guan ¹

¹ Jiangsu Provincial Key Laboratory of Geographic Information Science and Technology, School of Geographic and Oceanographic Sciences, Nanjing University, Nanjing 210023, China; chrisplum@smail.nju.edu.cn (T.C.); zhongqingguan@gmail.com (Z.G.)

² Nanjing Information Center, Nanjing 210019, China; hejun@njnet.gov.cn

³ School of the Environment, Nanjing University, Nanjing 210023, China; glxiaowei123@163.com

* Correspondence: gisjf@nju.edu.cn; Tel.: +86-25-8968-1296

Academic Editor: Yu-Pin Lin

Received: 23 June 2016; Accepted: 5 September 2016; Published: 16 September 2016

Abstract: The serious air pollution problem has aroused widespread public concerns in China. Nanjing city, as one of the famous cities of China, is faced with the same situation. This research aims to investigate spatial and temporal distribution characteristics of fine particulate matter (PM_{2.5}) and the influence of weather factors on PM_{2.5} in Nanjing using Spearman-Rank analysis and the Complete Ensemble Empirical Mode Decomposition with Adaptive Noise (CEEMDAN) method. Hourly PM_{2.5} observation data and daily meteorological data were collected from 1 April 2013 to 31 December 2015. The spatial distribution result shows that the Maigaoqiao site suffered the most serious pollution. Daily PM_{2.5} concentrations in Nanjing varied from 7.3 µg/m³ to 336.4 µg/m³. The highest concentration was found in winter and the lowest in summer. The diurnal variation of PM_{2.5} increased greatly from 6 to 10 a.m. and after 6 p.m., while the concentration exhibited few variations in summer. In addition, the concentration was slightly higher on weekends compared to weekdays. PM_{2.5} was found to exhibit a reversed relation with wind speed, relative humidity, and precipitation. Although temperature had a positive association with PM_{2.5} in most months, a negative correlation was observed during the whole period. Additionally, a high concentration was mainly brought with the wind with a southwest direction and several relevant factors are discussed to explain the difference of the impacts of diverse wind directions.

Keywords: PM_{2.5}; spatial and temporal variations; meteorological factors; CEEMDAN; Nanjing

1. Introduction

In recent years, the air pollution problem brought by rapid economic and unprecedented urbanization construction in China has aroused widespread public concerns, especially the fine particulate matter (PM_{2.5}) pollution, owing to the potential threats to health [1–3]. High PM_{2.5} concentration played an important role in the emergence of haze [4], which may account for the occurrence of extreme haze events in China in recent years [5,6]. Since aerodynamic diameter is less than 2.5 µm, PM_{2.5} can stay in the air for a long time and attach to harmful substances. Hence, long time exposure to PM_{2.5} concentration can lead to a significant impact on human health or even mortality [7–11].

Recently, a large number of studies paid attention to air suspended particulate matter (PM), especially PM_{2.5}, including emission sources, physical characteristics, and chemical decomposition [12–16]. A better and clearer understanding of spatial and temporal variations of PM_{2.5} can contribute to the adoption

of effective measures to reduce air pollution. Most research on the spatial and temporal distribution of $PM_{2.5}$ were obtained from a remote sensing map in China [17,18]. However, real-time monitoring data is essential to better obtain the detailed variations (seasonal, monthly, and diurnal) on the city scale. For example, Zhang et al. investigated the spatial-temporal $PM_{2.5}$ distribution characters of 190 cities in China [19]; Wang et al. analyzed the spatial and temporal variations of air pollutants at the 31 provincial capital cities of China [20]. Several studies have confirmed that meteorological variables play an important role in the formation of $PM_{2.5}$ as well as other factors like population and emissions etc. For instance, Zhang et al. explored spatiotemporal patterns of $PM_{2.5}$ and the determinants in 190 Chinese cities [21]. Yan et al. and Huang et al. also observed spatial and temporal variations of air pollutants including $PM_{2.5}$ and the relationship with meteorological factors [22,23].

The Yangtze River Delta (YRD), one of the most developed and fastest urbanized areas in China, has been facing a serious air pollution problem for the past ten years [24,25]. Air quality condition is also not optimistic in Nanjing city that is located in the western region of YRD. Deng et al. found that the annual average visibility in Nanjing was just 8.8 km and a daily average value of less than 10 km occurred on 57.9% of the days in 2004 [26]. According to the statistics of the meteorological department in Nanjing, the occurrence of haze days was 242 days in 2013, reaching the highest value in historical meteorological records [27]. In addition, rare rose red smog and haze phenomenon in the winter of 2015 attracted national attention for $PM_{2.5}$ pollution [28]. In Nanjing, many studies involving $PM_{2.5}$ mainly focused on heavy metals and chemical decomposition [29–31]. However, there were very limited studies that paid attention to the spatial-temporal distributions of $PM_{2.5}$ and its relation to meteorological conditions in the city. Shen et al. reported that the 24 h average $PM_{2.5}$ varied from $33 \mu\text{g}/\text{m}^3$ to $234 \mu\text{g}/\text{m}^3$ at a residential site in 2012 [32]. The purpose of this paper is to comprehensively explore the spatial-temporal variations of $PM_{2.5}$ and relationships between $PM_{2.5}$ and meteorological factors in Nanjing, using Spearman-Rank analysis and a new time-series data decomposition method: Complete Ensemble Empirical Mode Decomposition with Adaptive Noise (CEEMDAN).

2. Materials and Methods

2.1. Site Description and Data

Nanjing, the capital city of Jiangsu Province, is one of the ancient cities in China and has a rich historical and cultural heritage. As an intense industrialized and urbanized city with a forest coverage rate of over 35%, Nanjing is still facing a serious environmental pollution problem. There are nine monitoring sites defined by the China Environmental Monitoring Center (CEMC). All the monitoring sites are located in the urban area of Nanjing (Figure 1). Therefore, the research was carried out in the urban area. The hourly monitoring data of $PM_{2.5}$ used in the study were collected from the CEMC [33] from 1 April 2013 to 31 December 2015. In addition, the daily meteorological data were obtained from the China Meteorological Data Network [34] during the same period, including wind speed, temperature, relative humidity, precipitation, and wind direction.

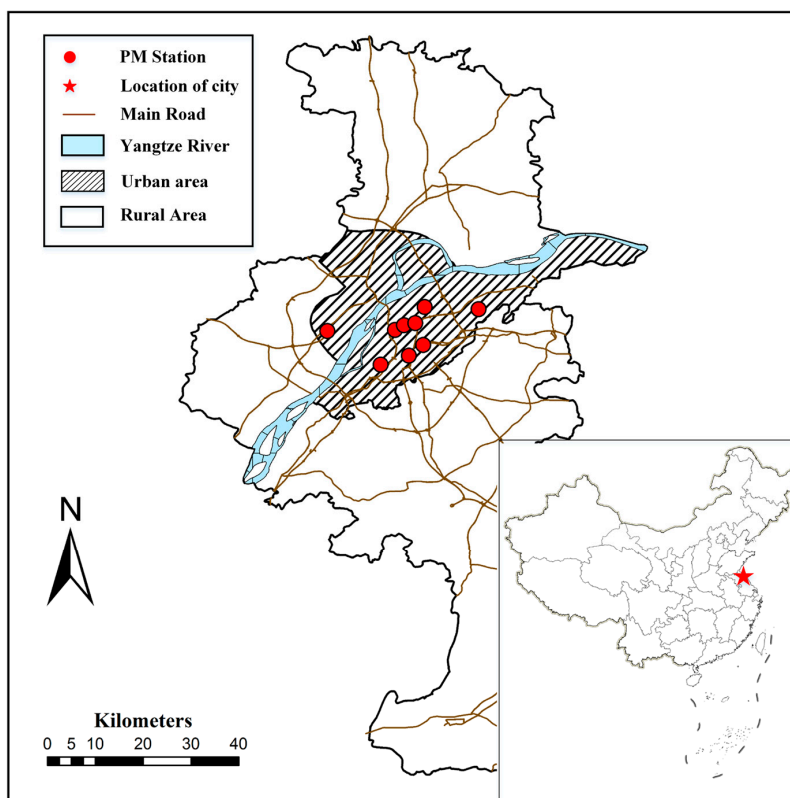


Figure 1. Map depicting the location of Nanjing in China (red star), air quality stations (red circles) and the distribution of main roads, urban areas, and rural areas. The corresponding $PM_{2.5}$ monitoring sites are: Pukou, Caochangmen, Shanxilu, Xuanwuhu, Maigaoqiao, Xianlindaxuecheng, Aotizhongxin, Zhonghuamen, and Ruijinlu (from left to right: six above and three below).

2.2. Methods

2.2.1. Analysis of Spatial and Temporal Variations

ArcGIS [35] and cluster analysis [36] were usually carried out to explore the spatial variation of $PM_{2.5}$ concentration. ArcGIS is simpler and more intuitive while the cluster analysis method requires repeatedly looking for the optimal cluster numbers. In this paper, ArcGIS was adopted to exhibit the region distribution of $PM_{2.5}$ mass concentration in Nanjing. Mean concentration of each site of the studied period (1 April 2013 to 31 December 2015) was calculated, and ArcGIS 10.2 software (Esri, Redlands, CA, USA) was utilized to explore the distribution of $PM_{2.5}$ in the urban area of Nanjing. Moreover, data processing was performed to obtain seasonal, monthly, and daily variations of $PM_{2.5}$ concentrations. In addition, a valid check on hourly data was conducted to get rid of the problematic data points before data processing tasks, and all data processing tasks above were conducted with Python.

2.2.2. CEEMDAN Decomposition

Complete Ensemble Empirical Mode Decomposition (CEEMDAN) is a new powerful decomposition and analysis method for time series data by Torres et al. [37]. It is able to better decompose the input signal into a collection of intrinsic mode functions (IMFs) without prior knowledge. Each decomposition component includes specific timescale information, where the residual IMF represents the trend of the signal data. Furthermore, CEEMDAN method was improved by Ensemble Empirical Mode Decomposition (EEMD) [38] that solved the mode mixing problem of Empirical Mode Decomposition (EMD) [39] and can better decompose different IMFs in frequency scale with the best completeness

and robustness. Although CEEMD is similar to Fourier analysis and wavelet decomposition, it could be used more simply and easily. This is because Fourier analysis requires sine and cosine function selection and wavelet analysis requires a wavelet basis.

According to EMD [39], each IMF should meet two conditions: (1) the difference of the number of zero-crossings related with the number of extrema must be no more than one; and (2) the average value of the envelopes computed by the local maxima and the local minima respectively is zero. The CEEMDAN method was carried out using the libeemd package [40], and the IMFs and residue of the daily PM_{2.5} concentration was calculated by performing the following steps:

- a Initialize signal $x(t) + \varepsilon_0 w^i(t)$, and decompose it by EMD to obtain their IMF_1 , where $x(t)$ is the daily PM_{2.5} mass concentration series and $w(t)$ is the appended white noise.
- b Compute first residue in the first cycle: $r_1(t) = x(t) - IMF_1(t)$.
- c Decompose i -th $r_1(t) + \varepsilon_1 E_1(w^i(t))$, until their IMF_1 of EMD and define IMF_2 , where $E_j(\cdot)$ produce the j -th mode obtained by EMD for the given signal.
- d Calculate k -th residue by $r_k(t) = r_{(k-1)}(t) - IMF_k(t)$.
- e Decompose i -th $r_k(t) + \varepsilon_k E_k(w^i(t))$ until their IMF_1 of EMD and define $(k + 1)$ -th IMF .
- f Repeat step d for the next k until the residue $R(t)$ has no more than two extrema.

Therefore, PM_{2.5} concentration signal $x(t)$ can be represented as:

$$x(t) = \sum_{k=1}^K IMF_k + R(t) \quad (1)$$

2.2.3. Relationship between PM_{2.5} and Meteorological Factors

Daily average PM_{2.5} data and daily mean meteorological data during the whole studied period were used in this section. Firstly, hourly PM_{2.5} monitoring data was processed to obtain daily mean data. Secondly, considering the climate characteristics of Nanjing city, twelve months were divided into: spring (March to May), summer (June to August), autumn (September to November), and winter (December to February). Thirdly, Spearman-Rank correlation analysis was utilized to study the correlations between PM_{2.5} concentration and meteorological variables (wind speed, temperature, relative humidity, precipitation, and wind direction). The analysis was conducted in each of four seasons and different months respectively. In order to fully understand the effect of wind direction with PM_{2.5} concentration, Box-Whiskers plot was depicted to explore the relationship between the concentration and wind direction. Additionally, data filtering work was also necessary for precipitation with at least 1 mm and Spearman-Rank analysis and Box-Whiskers plot were carried out in Python with the Pandas package.

3. Results and Discussion

3.1. PM_{2.5} Data Overview

Table 1 shows the summary of daily mean PM_{2.5} concentrations for nine sites in Nanjing. The daily average concentrations in Nanjing varied from 7.3 µg/m³ to 336.4 µg/m³, with a broader distribution. The lowest concentration was found in the Xuanwuhu site while the highest value was observed in the Aotizhongxin site. The results show that each site's median was much lower than mean, which means right-skewed distribution of PM_{2.5}. According to the World Health Organization's (WHO) recommended air quality guideline (AQG), 24 h average PM_{2.5} concentration should be less than 25 µg/m³, which is slightly lower than the grade-1 level (35 µg/m³) of China's national ambient air quality standards [10,41]. Due to the relatively relaxed standard, interim targets (ITs) were simultaneously recommended for the developing countries, including IT-1 (75 µg/m³), IT-2 (50 µg/m³) and IT-3 (37.5 µg/m³) [42]. The percentage of daily average PM_{2.5} concentrations in Nanjing reaching the four recommended targets was 68.6%, 41.7%, 24.3% and 9.3%, respectively.

The differences of the percentage reaching the standard for each site were not obvious except for the AQG. Xianlindaxuecheng site had highest percentage matching four targets, followed by Xuanwuhu site. Moreover, the percentages for three ITs at the Maigaoqiao site were the lowest, indicating the most serious PM_{2.5} pollution.

Table 1. The summary of daily average fine particulate matter (PM_{2.5}) concentrations for nine monitoring sites.

Station	Basic Statistic (µg/m ³)					Percentage Reaching for Standard ¹ (%)			
	Max.	Mean	Median	Min.	Std.	IT-1	IT-2	IT-3	AQG
Aotizhongxin	373.3	68.4	58.0	2.0	46.8	67.6	41.4	24.5	9.5
Caochangmen	353.1	66.9	56.9	4.0	43.4	69.6	41.4	24.5	9.0
Maigaoqiao	327.7	70.4	61.0	8.7	43.0	64.8	35.6	21.0	6.6
Pukou	336.0	67.0	57.5	2.7	42.5	67.7	40.9	23.8	7.8
Ruijinlu	338.0	68.1	58.0	9.7	42.1	69.6	40.3	23.8	4.3
Shanxilu	332.6	65.0	55.4	6.1	42.7	70.6	44.3	27.1	11.6
Xianlindaxuecheng	319.5	63.2	53.0	3.0	45.6	72.0	46.3	31.5	15.3
Xuanwuhu	366.7	63.2	54.0	1.0	44.5	70.8	46.2	29.8	14.3
Zhonghuamen	303.0	64.1	56.0	4.8	39.3	71.5	43.5	26.4	10.4

¹ World Health Organization (WHO) (2006) recommends the air quality guideline (AQG, 25 µg/m³) and three interim targets (IT-1, 75 µg/m³; IT-2, 50 µg/m³; IT-3, 37.5 µg/m³).

3.2. Regional Variation

Figure 2 shows the spatial distribution of the average PM_{2.5} concentrations for each monitoring site of Nanjing in the past three years. The map shows that PM_{2.5} pollution was most serious at Maigaoqiao, followed by Aotizhongxin and Ruijinlu. The finest air quality was observed at Xuanwuhu and Xianlindaxuecheng. In order to exhaustively explain the spatial distribution of PM_{2.5}, the typical characteristics of the nine monitoring sites in Nanjing were collected in Table 2. According to the information shown in Table 2, Maigaoqiao had the worst environment, and the main sources of pollution found at the Aotizhongxin site came from urban construction activities while Ruuijinlu station is located in a dense residential area; on the contrary, Xuanwuhu and Xianlindaxuecheng sites owe their superior environment to the lack of big emissions of particulate pollutants. Through the above analysis, spatial distribution was closely related to geographical location. Meanwhile, due to the systematic information of particulate matter pollution, the impact of terrain, vegetation cover, and weather conditions cannot be ignored in the process.

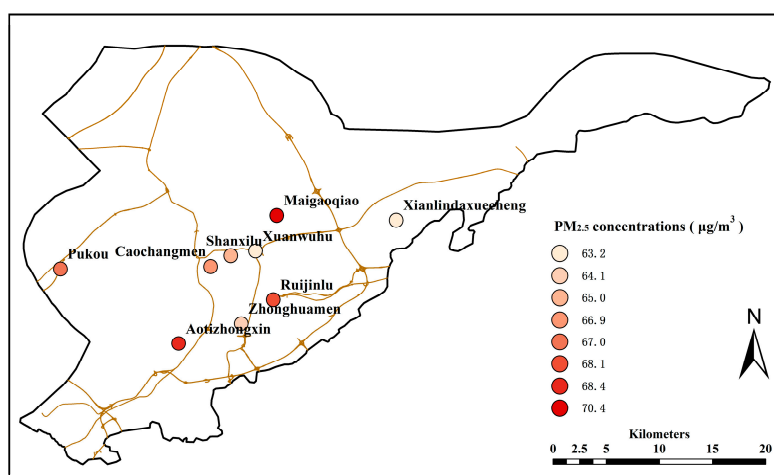


Figure 2. Regional distribution of the average PM_{2.5} mass concentrations in the past three years in Nanjing.

Table 2. The typical characteristics for each particulate matter (PM) monitoring station in Nanjing city.

Station	Main Activities and Characteristics around Station
Aotizhongxin	New city area, frequent urban construction activities
Caochangmen	Adjacent to the Yangtze River, around the universities, tourism
Maigaoqiao	Once urban-rural binding region, frequent urban construction activities, petrochemical technology, thermal power plant
Pukou	Nanjing Laoshan National Forest Park (station inside), dense construction activities, tourism
Ruijinlu	Dense residential area, tourism
Shanxilu	Residential area, shopping center
Xianlindaxuecheng	University area, shopping malls
Xuanwuhu	Xuanwuhu Lake (largest city park in the Jiangnan region), tourism
Zhonghuamen	Traffic arteries, tourism

3.3. Temporal Variation

Seasonal variations of PM_{2.5} concentrations for all sites in Nanjing are shown in Figure 3, where April and May were only included in the spring and December was included in the winter in 2013. PM_{2.5} pollution in the winter was much more severe than other seasons, especially in 2013, with the average value of up to 158.5 μg/m³. Normally, it is followed by spring (63.1 μg/m³) and autumn (59.9 μg/m³). The finest air quality appeared in the summer and the concentration value in the summer of 2014 (64.8 μg/m³) was higher than in 2013 (44.7 μg/m³) and 2015 (38.8 μg/m³). It can be seen from the statistics of standard deviation that the pollution condition of PM_{2.5} was most turbulent in the winter of 2013, consistent with the above analysis. In addition, the concentration in 2015 was significantly lower than in 2013 or in 2014.

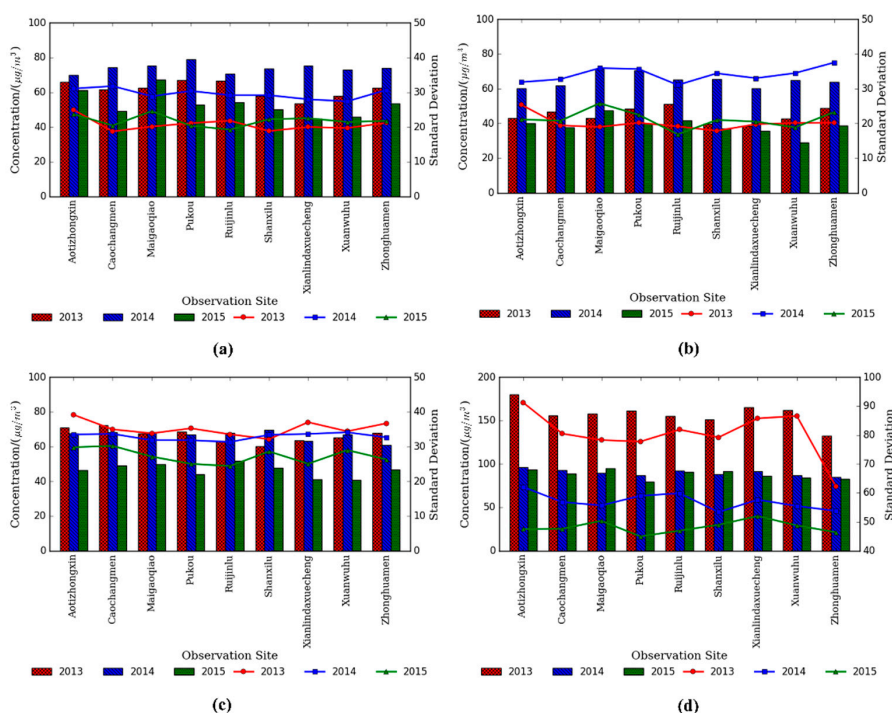


Figure 3. Seasonal variation of PM_{2.5} concentrations for the past three years in Nanjing. The bar represents the concentration of PM_{2.5} and the line means standard deviation; (a) Spring; (b) Summer; (c) Autumn and (d) Winter.

Figure 4 shows monthly variation of PM_{2.5} concentrations in Nanjing. For 2014, the highest PM_{2.5} concentration appeared in January. In addition, the concentration in February, March, and April continually decreased. There was a sharp rise of PM_{2.5} concentration in May, and the value in June was a little higher than in May. Subsequently, the concentration value reduced in the next two months. The lowest concentration of the whole year was observed in August, and the average value was 42.4 µg/m³, which is very close to the grade-1 value (32 µg/m³) national standard [41]. The concentration continued to increase in September, October and November. However, a rare decline occurred in December. Monthly variation in 2013 and 2015 was basically analogous to that in 2014, but several differences were observed: the lowest average value was found in July of 2013 and September of 2015; the concentration continually increased from October to December in both 2013 and 2015, different from the decrease in December of 2014; PM_{2.5} pollution was the highest for the studied period in the winter of 2013, followed by January in 2014, indicating that pollution was on going.

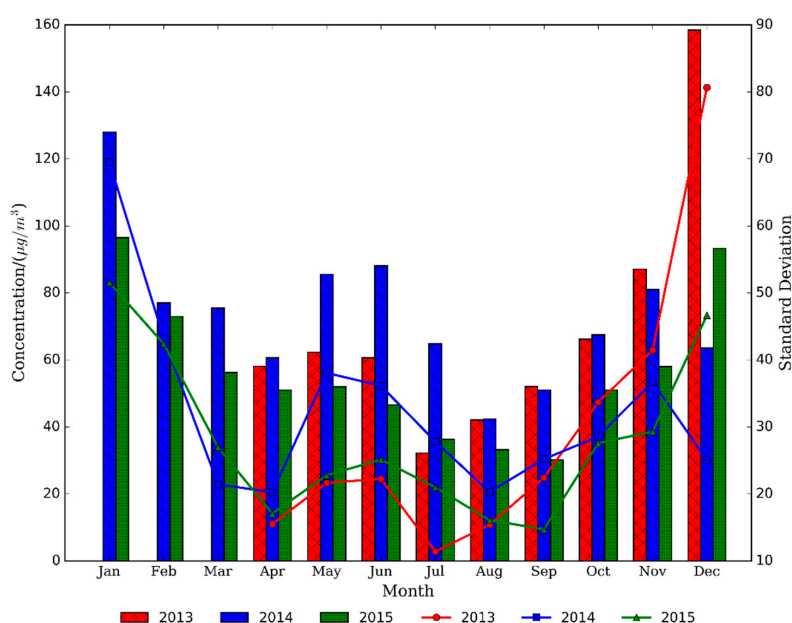


Figure 4. Monthly variation of PM_{2.5} concentrations in Nanjing. The bar represents PM_{2.5} concentrations and the line means standard deviation.

According to the analysis results of the Nanjing Environmental Protection Bureau [43], the main factors influencing PM_{2.5} pollution are fired coal and industrial production. Fired coal from plants and industry and dust from industrial areas and construction sites can account for the most serious pollution problems in the winter. Following the strengthening energy conservation and reduction of pollution emissions from 2014, it was unexpected to find that the concentration in December of 2015 was instead higher than that in 2014. Through checking the meteorological records, low frequency and the weak intensity of cold air in 2015 led to the above contrast.

Figure 5 shows diurnal variation of PM_{2.5} for different seasons and different years in Nanjing. For seasons, the diurnal variation of PM_{2.5} concentrations in winter was higher than other seasons. It is followed by spring, autumn, and summer, which verifies the information in Figure 3. The concentration value increased significantly from 6:00 to 10:00 in the morning and after 6:00 in the evening, except in summer, where the rush hour in the morning of winter was found from 8:00 to 10:00 a.m. This means rush hour traffic emissions are of importance to PM_{2.5} concentration variation. In summer, rush hour peaked in the morning (6:00–11:00 a.m.) and PM concentration had few changes at other times of the day. In terms of years, the diurnal variation for each year showed similar trends, and PM_{2.5} concentrations of each hour in 2015 was clearly lower than in 2013 and 2014, which confirms that air quality has been improved. Due to the decline of anthropogenic emissions and favorable

meteorological conditions, the value of PM_{2.5} was continually reduced from noon to afternoon/early evening. Frequent temperature inversion and the lowest height of mixing layer from the evening to the early morning are not beneficial to the vertical diffusion of pollutants [44], which contributes to the relatively high PM_{2.5} concentration in the early morning.

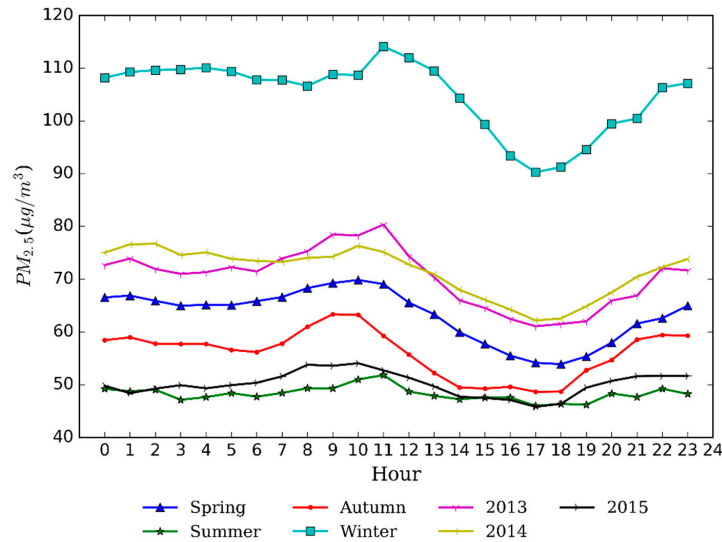


Figure 5. Diurnal variation of PM_{2.5} concentrations in Nanjing.

Figure 6 shows average weekday and weekend variations of PM_{2.5} concentrations for the whole period in Nanjing. The mean concentration was slightly higher on weekends (67.7 µg/m³) than that on weekdays (63.0 µg/m³). This may be owing to temporary increase in the intensity of urban construction activities on weekends while those activities are restricted on weekdays. In addition, the largest differences (about 10 µg/m³) were only found at a few moments while most of daytime had small differences in concentration. It follows that there was no obvious variation between weekdays and weekends for PM_{2.5} concentrations in the studied period. Hu et al. also reported that PM_{2.5} concentrations in the YRD cities exhibited small variations on weekdays compared to weekends [45]. Furthermore, weekdays showed a similar trend pattern of PM_{2.5} concentration with weekends, but one hour later on weekends, indicating a change in human activities.

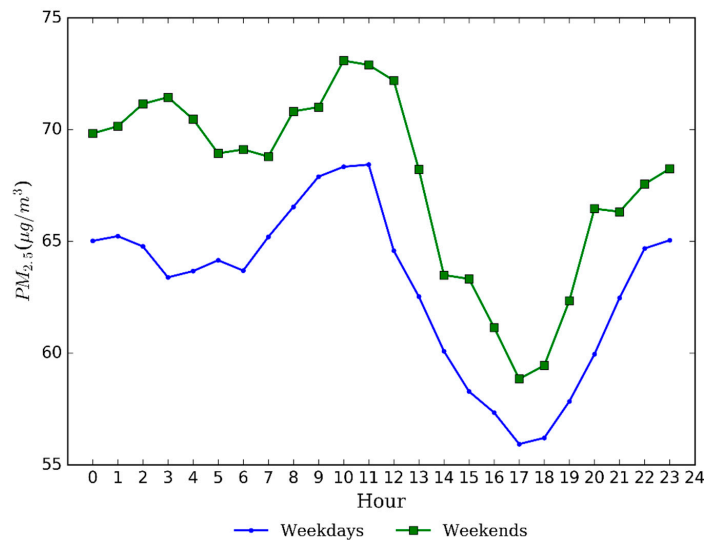


Figure 6. Weekday and weekend variations of PM_{2.5} concentrations in Nanjing.

3.4. Decomposition of Time Series Data

Figure 7 shows that variations in different time frequencies and the overall trend decomposed by the given signal of $PM_{2.5}$. Eight IMFs and one residue were obtained in the process. The results look similar but differ in amplitude and frequency. IMF1 has the highest amplitude and frequency, on the contrary, IMF8 has the lowest. When the results were stripped from the original signal, the trend of the whole period for the study was generated. As shown in the residue of Figure 7, the curve of the trend exhibits parabolic distribution. $PM_{2.5}$ concentration in 2015 shows a slight downward trend compared with that in 2014. The result is consistent with that in the Figure 3, which indicates that measures related to environmental protection have been successful. Due to the uncomplete data, we cannot obtain the overall trend for the whole year of 2013.

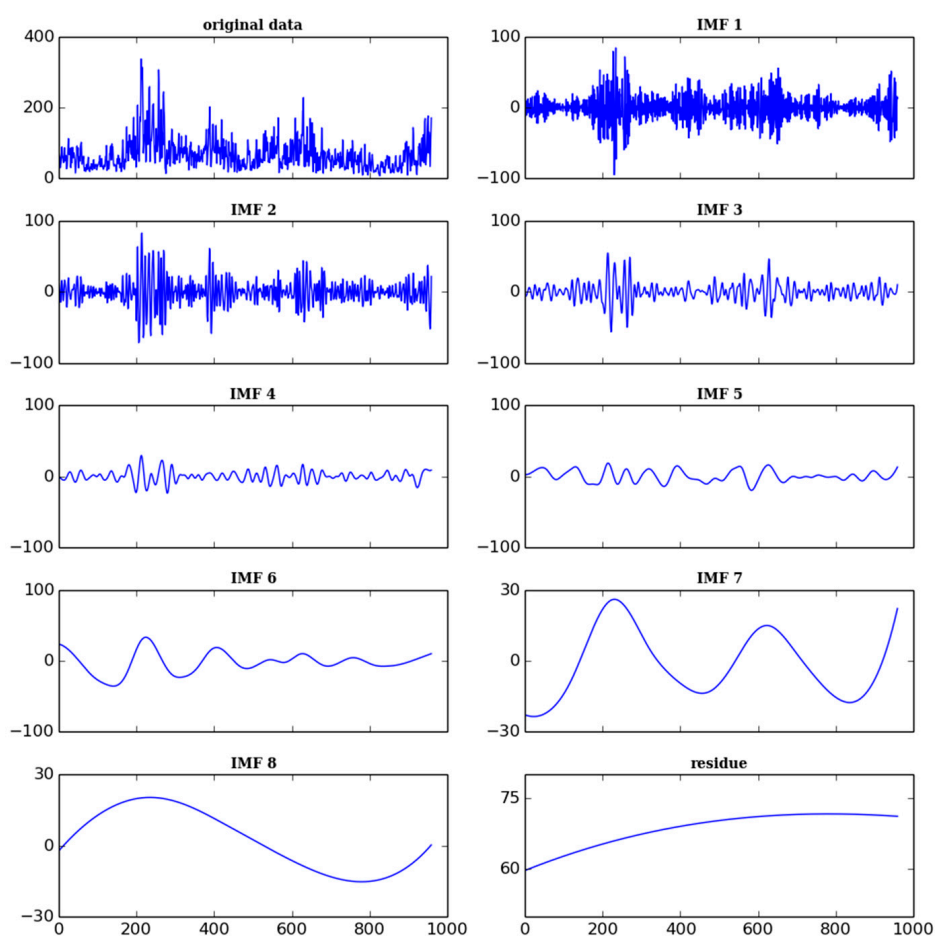


Figure 7. CEEMDAN decomposition of $PM_{2.5}$ concentrations for three years.

In general, low-frequency signals contain yearly variations while high frequency signals include sudden changes. IMFs from IMF1 to IMF6 mean the period less than a year while IMF8 represents inter-annual changes. In addition, the IMF7 represents the cycle of about a year. Therefore, the original signal was reconstructed by getting together the IMFs without IMF8 and the residue to obtain seasonal changes of $PM_{2.5}$ mass concentration in Nanjing. The mean concentration in each season was computed by averaging the reconstructed data series in the four seasons. Figure 8 shows the mean concentration in the different seasons of three years, where the data are not complete in the spring and winter of 2013. Several details can be seen: (1) the seasonal $PM_{2.5}$ concentration varied greatly; (2) the highest concentration was always found in winter while the lowest was in summer; and (3) the concentration in winter of 2015 was a little higher than in 2014.

Integrating the high frequency information in Figure 7, the number of days and the amplitude for sudden changes were significantly decreased in the same period. During the study period, sudden changes of $PM_{2.5}$ concentration mainly focused on January and December, especially in December of 2013. There are a variety of factors that cause an instant increase of $PM_{2.5}$ concentration [29,46], like fireworks, dust episodes, and gas heating. Fireworks occur mainly around the Spring Festival and lead to sudden increases in $PM_{2.5}$ concentration in the winter. Fired coal from plants is used throughout winter while dust episodes happen occasionally throughout the whole year.

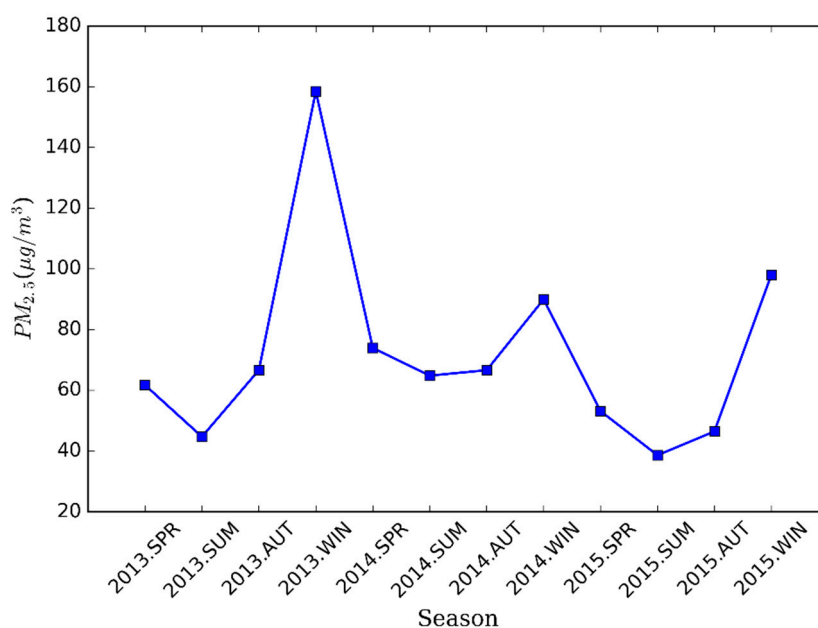


Figure 8. Seasonal distribution of $PM_{2.5}$ concentrations for three years based on the CEEMDAN decomposition results.

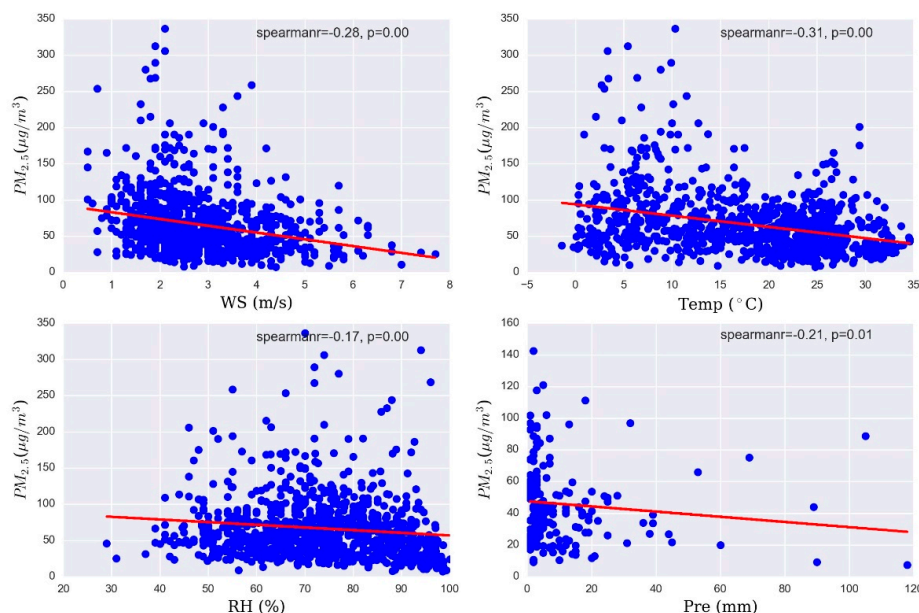
3.5. Correlation between $PM_{2.5}$ and Meteorological Factors

Table 3 shows that the correlation coefficients of $PM_{2.5}$ concentration related with wind speed, temperature, relative humidity, and precipitation using the Spearman-Rank analysis method. A negative relationship was weakly exhibited among $PM_{2.5}$ and wind speed in the season months, which does not match a similar study [47]. The most possible reason is the effect of mountainous terrain on the wind in the urban area. Temperature positively correlated with $PM_{2.5}$ in most months. This is because high temperature contributes to photochemical activity to produce more secondary particles [48]. Relative humidity had a strong negative association with $PM_{2.5}$ in summer. Very high humidity can make suspended particles get together, then particles cannot stay in the air and fall to the ground to cause the decrease of $PM_{2.5}$ concentrations. Precipitation showed strongly reverse correlation with $PM_{2.5}$ in February and winter. In order to better explore the overall effects of meteorological variables, Spearman-Rank correlations between $PM_{2.5}$ concentration and weather conditions are shown in Figure 9. Wind speed, relative humidity, and precipitation had weak negative associations with $PM_{2.5}$ concentrations. However, a negative relationship was found between temperature and $PM_{2.5}$ during the whole period. The above analysis results make us believe that the influence of meteorological parameters is a very complex and comprehensive process. Therefore, more detailed study is needed to analyze the impact of weather conditions on $PM_{2.5}$ concentration in the future, such as adding hourly meteorological data and exploring multiple relationships.

Table 3. The correlation coefficients of daily PM_{2.5} related with meteorological variables.

Month/Season	WS	T	RH	Pre
January	−0.07	0.53 **	−0.01	−0.43
February	−0.22	0.35 **	−0.17	−0.76 **
March	−0.06	0.43 **	0.06	−0.39
April	−0.23	0.28 *	−0.04	0.32
May	−0.41 **	0.41 **	−0.17	−0.27
June	−0.37 **	0.34 **	−0.23 *	−0.23
July	−0.36 **	−0.02	−0.06	0.05
August	−0.35 **	0.33 **	−0.45 **	0.07
September	−0.36 **	0.35 **	0.05	−0.35
October	−0.30 **	−0.03	−0.10	−0.28
November	−0.38 **	0.35 **	−0.34 **	−0.26
December	−0.16	0.29 **	0.28 **	−0.80
Winter	−0.17	0.35 **	0.02	−0.67 **
Spring	−0.26 **	0.22 **	−0.05	−0.17
Summer	−0.26 **	−0.03	−0.60 *	−0.05
Autumn	−0.38 **	−0.26 **	−0.19 **	−0.28

Note: WS, Wind Speed; T, Temperature; RH, Relative Humidity; Pre, Precipitation; * $p < 0.05$; ** $p < 0.01$.

**Figure 9.** The relationship between PM_{2.5} concentrations and meteorological conditions.

3.6. Effect of Wind Direction on PM_{2.5} Concentration

As an important meteorological factor, the role of wind direction cannot be ignored [49]. PM_{2.5} concentration related with specific wind direction is presented in Figure 10. The figure shows that southwest wind led to the highest PM concentration, followed by north wind and northwest wind. Remarkably, such a result is not consistent with what people had expected, that is, owing to the industry pollution in the north region [20], the winds from north were expected to lead to high PM_{2.5} concentration, meanwhile southwest wind should not. However, the results were not as expected and there is a slight difference among north winds. There are several possible aspects to be discussed about this contrast. First, there is a big iron and steel industry zone close to the urban area in the southwest of Nanjing and the base of Ma'anshan iron and steel industry is also located in the direction adjacent to Nanjing city. Therefore, large amount of particles generated from the industry can spread to urban areas by a southwest wind, which directly aggravates the PM_{2.5} pollution. Second, particles can

be transported into Nanjing from the north region, which could be confirmed by the trajectories of air flows using the HYSPLIT model in Figure 11. Nonetheless, with the transportation of pollutants, cold air is usually brought by air flows directly from the north and then it encounters the warm flows from south in the Nanjing area. In the process, favorable weather conditions can be formed and directly lead to the attenuation of PM_{2.5}, which cause unremarkable PM_{2.5} pollution by winds with north directions. Meanwhile, due to the mountain terrain in the northwest, it is not beneficial to the horizontal diffusion of air pollutants and leads to higher PM_{2.5} concentration related with northwest wind. Additionally, the result might partly verify the preliminary analysis of the pollution source that PM_{2.5} pollution is mainly derived from local pollution while regional transportation was responsible for about 28.5% [43]. Certainly, the analysis of wind direction involves many factors, such as pollution sources, terrain, mixing layer, etc., and due to the limited data, basic analysis is only given for the statistic result in this section.

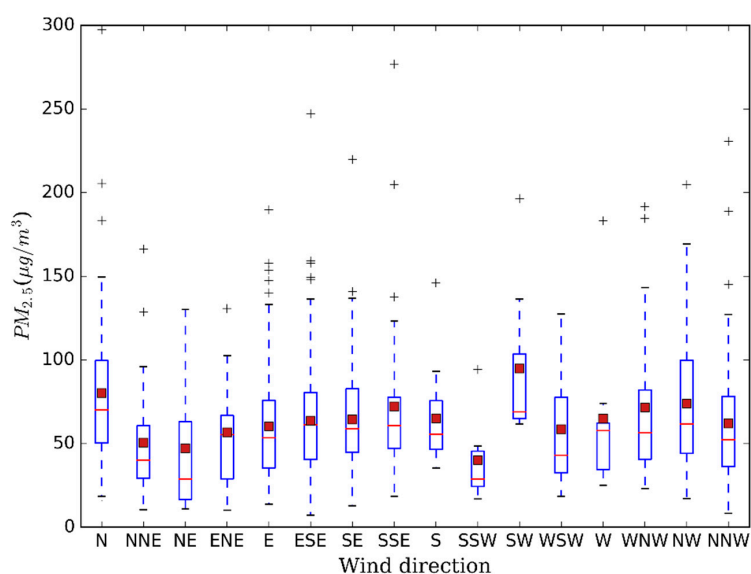


Figure 10. Box-Whiskers plot of PM_{2.5} mass concentration related with wind direction. Bottom and top of the blue box represent 25th and 75th percentile, whereas bottom and top of the vertical dotted line mean minimum and maximum value. The red solid lines represent median value and the firebrick square represent mean value. Outliers are depicted by the “+”.

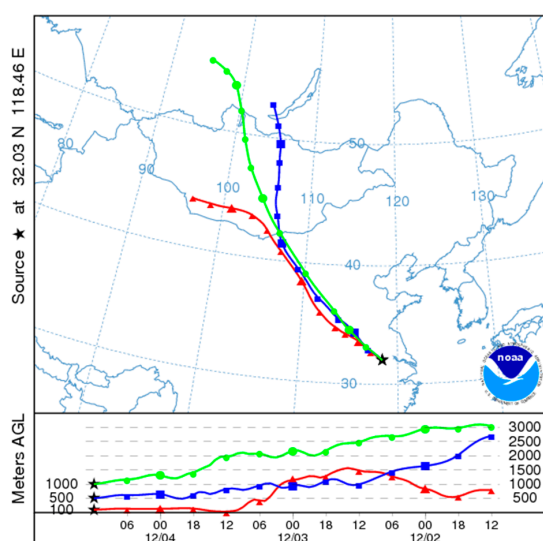


Figure 11. Analysis of the back trajectories of air flows for the 72 h cycle in the winter of 2014 based on the meteorological data of Global Data Assimilation System (GDAS).

4. Conclusions

Spatial-temporal variations of PM_{2.5} and its relation with meteorological variables in Nanjing were analyzed in the paper and several conclusions can be drawn as follows:

- (a) Daily average PM_{2.5} concentration varied from 7.3 µg/m³ to 336.4 µg/m³. The ArcGIS map shows that Maigaoqiao suffered the poorest air quality, followed by Aotizhongxin and Ruijinlu. The lowest concentration was found at the Xuanwuhu site. The results show that spatial distribution of PM_{2.5} is not only related to geographical location but also other factors.
- (b) Seasonal variation of PM_{2.5} was obvious and the highest concentration was found in winter while the lowest occurred in summer. The diurnal PM_{2.5} concentration increased significantly from 6:00 to 10:00 in the morning and after 6:00 in the evening and stayed relatively high in the early morning. There was no significant weekend effect in Nanjing city. The CEEMDAN decomposition results show that the frequency and intensity of sudden change decreased year by year and there was a decreasing trend from 2014.
- (c) Spearman-Rank analysis was involved to explore the relationship between PM_{2.5} and meteorological factors. PM_{2.5} exhibited a negative association with wind speed, relative humidity, and precipitation. Temperature positively correlated with PM_{2.5} in most months but showed a negative correlation during the whole period, indicating a complex influence. In addition, high PM_{2.5} concentration was mainly related to southwest wind.

There are still several phenomena that need comprehensive study, such as the influence of meteorological factors including mixing layer and the effect of terrain on PM concentration related to wind. It is also worth further exploring the differences of PM_{2.5} mass concentration between urban areas and rural areas in Nanjing city. The content mentioned above will be taken into account in a future study.

Acknowledgments: This work was supported by the National Natural Science Foundation of China under Grant No. 41371365 and National Natural Science Foundation of China under Grant No. 41230751.

Author Contributions: Jiangfeng She conceived the experiment and edited the manuscript; Tao Chen performed the task of data processing, analyzed the results, and wrote the manuscript. Jun He and Xiaowei Lu were involved in the analysis process. Zhongqing Guan partially contributed to the data processing work.

Conflicts of Interest: The authors declare no conflict of interest.

References

1. Wang, S.; Hao, J. Air quality management in China: Issues, challenges, and options. *J. Environ. Sci.* **2012**, *24*, 2–13. [[CrossRef](#)]
2. Han, L.J.; Zhou, W.Q.; Li, W.F.; Li, L. Impact of urbanization level on urban air quality: A case of fine particles (PM_{2.5}) in Chinese cities. *Environ. Pollut.* **2014**, *194*, 163–170. [[CrossRef](#)] [[PubMed](#)]
3. Zhang, F.; Cheng, H.R.; Wang, Z.W.; Lv, X.P.; Zhu, Z.M.; Zhang, G.; Wang, X.M. Fine particles (PM_{2.5}) at a CAWNET background site in Central China: Chemical compositions, seasonal variations and regional pollution events. *Atmos. Environ.* **2014**, *86*, 193–202. [[CrossRef](#)]
4. Liu, Y.-J.; Zhang, T.-T.; Liu, Q.-Y.; Zhang, R.-J.; Sun, Z.-Q.; Zhang, M.-G. Seasonal variation of physical and chemical properties in TSP, PM₁₀ and PM_{2.5} at a roadside site in Beijing and their influence on atmospheric visibility. *Aerosol Air Qual. Res.* **2014**, *14*, 954–969. [[CrossRef](#)]
5. Huang, R.-J.; Zhang, Y.; Bozzetti, C.; Ho, K.-F.; Cao, J.-J.; Han, Y.; Daellenbach, K.R.; Slowik, J.G.; Platt, S.M.; Canonaco, F. High secondary aerosol contribution to particulate pollution during haze events in China. *Nature* **2014**, *514*, 218–222. [[CrossRef](#)] [[PubMed](#)]
6. Zhao, X.; Zhao, P.; Xu, J.; Meng, W.; Pu, W.; Dong, F.; He, D.; Shi, Q. Analysis of a winter regional haze event and its formation mechanism in the North China Plain. *Atmos. Chem. Phys.* **2013**, *13*, 5685–5696. [[CrossRef](#)]

7. Bell, M.L.; Dominici, F.; Ebisu, K.; Zeger, S.L.; Samet, J.M. Spatial and temporal variation in PM_{2.5} chemical composition in the United States for health effects studies. *Environ. Health Perspect.* **2007**, *115*, 989–995. [[CrossRef](#)] [[PubMed](#)]
8. Dockery, D.W.; Pope, C.A.; Xu, X.; Spengler, J.D.; Ware, J.H.; Fay, M.E.; Ferris, B.G., Jr.; Speizer, F.E. An association between air pollution and mortality in six U.S. cities. *N. Engl. J. Med.* **1993**, *329*, 1753–1759. [[CrossRef](#)] [[PubMed](#)]
9. Pope, C.A., III; Burnett, R.T.; Thun, M.J.; Calle, E.E.; Krewski, D.; Ito, K.; Thurston, G.D. Lung cancer, cardiopulmonary mortality, and long-term exposure to fine particulate air pollution. *JAMA* **2002**, *287*, 1132–1141. [[CrossRef](#)] [[PubMed](#)]
10. Burden of Disease from Household Air Pollution for 2012. Available online: http://www.who.int/phe/health_topics/outdoorair/databases/FINAL_HAP_AAP_BoD_24March2014.pdf?ua=1 (accessed on 10 March 2016).
11. Chen, Z.; Wang, J.N.; Ma, G.X.; Zhang, Y.S. China tackles the health effects of air pollution. *Lancet* **2013**, *382*, 1959–1960. [[CrossRef](#)]
12. Xiao, Z.; Bi, X.; Feng, Y.; Wang, Y.; Zhou, J.; Fu, X.; Weng, Y. Source apportionment of ambient PM₁₀ and PM_{2.5} in urban area of Ningbo city. *Res. Environ. Sci.* **2012**, *25*, 549–555.
13. Sun, Y.W.; Zhou, X.H.; Wai, K.M.; Yuan, Q.; Xu, Z.; Zhou, S.Z.; Qi, Q.; Wang, W.X. Simultaneous measurement of particulate and gaseous pollutants in an urban city in North China Plain during the heating period: Implication of source contribution. *Atmos. Res.* **2013**, *134*, 24–34. [[CrossRef](#)]
14. Wang, Z.; Hu, M.; Wu, Z.; Yue, D.; He, L.; Huang, X.; Liu, X.; Wiedensohler, A. Long-term measurements of particle number size distributions and the relationships with air mass history and source apportionment in the summer of Beijing. *Atmos. Chem. Phys.* **2013**, *13*, 10159–10170. [[CrossRef](#)]
15. Ma, J.; Chen, Z.; Wu, M.; Feng, J.; Horii, Y.; Ohura, T.; Kannan, K. Airborne PM_{2.5}/PM₁₀-associated chlorinated polycyclic aromatic hydrocarbons and their parent compounds in a suburban area in Shanghai, China. *Environ. Sci. Technol.* **2013**, *47*, 7615–7623. [[CrossRef](#)] [[PubMed](#)]
16. Yuan, Q.; Yang, L.; Dong, C.; Yan, C.; Meng, C.; Sui, X.; Wang, W. Particle physical characterisation in the Yellow River Delta of Eastern China: Number size distribution and new particle formation. *Air Qual. Atmos. Health* **2015**, *8*, 441–452. [[CrossRef](#)]
17. Ma, Z.; Hu, X.; Sayer, A.M.; Levy, R.; Zhang, Q.; Xue, Y.; Tong, S.; Bi, J.; Huang, L.; Liu, Y. Satellite-based spatiotemporal trends in PM_{2.5} concentrations: China, 2004–2013. *Environ. Health Perspect.* **2015**, *124*, 184–192. [[CrossRef](#)] [[PubMed](#)]
18. Ma, Z.; Liu, Y.; Zhao, Q.; Liu, M.; Zhou, Y.; Bi, J. Satellite-derived high resolution PM_{2.5} concentrations in Yangtze River Delta Region of China using improved linear mixed effects model. *Atmos. Environ.* **2016**, *133*, 156–164. [[CrossRef](#)]
19. Zhang, Y.L.; Cao, F. Fine particulate matter (PM_{2.5}) in China at a city level. *Sci. Rep.* **2015**, *5*, 14884. [[CrossRef](#)] [[PubMed](#)]
20. Wang, Y.G.; Ying, Q.; Hu, J.L.; Zhang, H.L. Spatial and temporal variations of six criteria air pollutants in 31 provincial capital cities in China during 2013–2014. *Environ. Int.* **2014**, *73*, 413–422. [[CrossRef](#)] [[PubMed](#)]
21. Zhang, H.; Wang, Z.; Zhang, W. Exploring spatiotemporal patterns of PM_{2.5} in China based on ground-level observations for 190 cities. *Environ. Pollut.* **2016**. [[CrossRef](#)] [[PubMed](#)]
22. Yan, S.; Cao, H.; Chen, Y.; Wu, C.; Hong, T.; Fan, H. Spatial and temporal characteristics of air quality and air pollutants in 2013 in Beijing. *Environ. Sci. Pollut. Res.* **2016**, *23*, 1–12. [[CrossRef](#)] [[PubMed](#)]
23. Huang, F.; Li, X.; Wang, C.; Xu, Q.; Wang, W.; Luo, Y.; Tao, L.; Gao, Q.; Guo, J.; Chen, S. PM_{2.5} spatiotemporal variations and the relationship with meteorological factors during 2013–2014 in Beijing, China. *PLoS ONE* **2015**, *10*, e0141642. [[CrossRef](#)] [[PubMed](#)]
24. Shi, C.; Yang, J.; Qiu, M.; Zhang, H.; Zhang, S.; Li, Z. Analysis of an extremely dense regional fog event in Eastern China using a mesoscale model. *Atmos. Res.* **2010**, *95*, 428–440. [[CrossRef](#)]
25. Ding, A.; Fu, C.; Yang, X.; Sun, J.; Zheng, L.; Xie, Y.; Herrmann, E.; Nie, W.; Petäjä, T.; Kerminen, V.-M. Ozone and fine particle in the western Yangtze River Delta: An overview of 1 yr data at the SORPES station. *Atmos. Chem. Phys.* **2013**, *13*, 5813–5830.

26. Deng, J.J.; Wang, T.J.; Jiang, Z.Q.; Xie, M.; Zhang, R.J.; Huang, X.X.; Zhu, J.L. Characterization of visibility and its affecting factors over Nanjing, China. *Atmos. Res.* **2011**, *101*, 681–691. [[CrossRef](#)]
27. Nanjing Meteorology Bureau. Available online: <http://www.njqxj.gov.cn/> (accessed on 26 August 2016).
28. Rose-Red Haze Show Nanjing. Available online: http://www.sh.xinhuanet.com/2015-12/23/c_134943910.htm (accessed on 26 August 2016).
29. Kong, S.; Li, X.; Li, L.; Yin, Y.; Chen, K.; Yuan, L.; Zhang, Y.; Shan, Y.; Ji, Y. Variation of polycyclic aromatic hydrocarbons in atmospheric PM_{2.5} during winter haze period around 2014 Chinese Spring Festival at Nanjing: Insights of source changes, air mass direction and firework particle injection. *Sci. Total Environ.* **2015**, *520*, 59–72. [[CrossRef](#)] [[PubMed](#)]
30. Hu, X.; Zhang, Y.; Ding, Z.; Wang, T.; Lian, H.; Sun, Y.; Wu, J. Bioaccessibility and health risk of arsenic and heavy metals (Cd, Co, Cr, Cu, Ni, Pb, Zn and Mn) in TSP and PM_{2.5} in Nanjing, China. *Atmos. Environ.* **2012**, *57*, 146–152. [[CrossRef](#)]
31. Cui, F.; Chen, M.; Ma, Y.; Zheng, J.; Yao, L.; Zhou, Y. Optical properties and chemical apportionment of summertime PM_{2.5} in the suburb of Nanjing. *J. Atmos. Chem.* **2016**, *73*, 119–135. [[CrossRef](#)]
32. Shen, G.F.; Yuan, S.Y.; Xie, Y.N.; Xia, S.J.; Li, L.; Yao, Y.K.; Qiao, Y.Z.; Zhang, J.; Zhao, Q.Y.; Ding, A.J. Ambient levels and temporal variations of PM_{2.5} and PM₁₀ at a residential site in the mega-city, Nanjing, in the western Yangtze River Delta, China. *J. Environ. Sci. Health Part A* **2014**, *49*, 171–178. [[CrossRef](#)] [[PubMed](#)]
33. China Environmental Monitoring Center. Available online: <http://113.108.142.147:20035/emcpublish/> (accessed on 20 March 2016).
34. China Meteorological Data Network. Available online: <http://data.cma.gov.cn/> (accessed on 20 March 2016).
35. Feng, X.; Li, Q.; Zhu, Y.; Wang, J.; Liang, H.; Xu, R. Formation and dominant factors of haze pollution over Beijing and its peripheral areas in winter. *Atmos. Pollut. Res.* **2014**, *5*, 528–538. [[CrossRef](#)]
36. Baxter, L.K.; Sacks, J.D. Clustering cities with similar fine particulate matter exposure characteristics based on residential infiltration and in-vehicle commuting factors. *Sci. Total Environ.* **2014**, *470*, 631–638. [[CrossRef](#)] [[PubMed](#)]
37. Torres, M.E.; Colominas, M.A.; Schlotthauer, G.; Flandrin, P. A complete ensemble empirical mode decomposition with adaptive noise. In Proceedings of the 2011 IEEE International Conference on Acoustics, Speech and Signal Processing (ICASSP), Prague, Czech Republic, 22–27 May 2011; pp. 4144–4147.
38. Wu, Z.; Huang, N.E. Ensemble empirical mode decomposition: A noise-assisted data analysis method. *Adv. Adapt. Data Anal.* **2009**, *1*, 1–41. [[CrossRef](#)]
39. Huang, N.E.; Shen, Z.; Long, S.R.; Wu, M.C.; Shih, H.H.; Zheng, Q.; Yen, N.-C.; Tung, C.C.; Liu, H.H. The empirical mode decomposition and the Hilbert spectrum for nonlinear and non-stationary time series analysis. *Proc. R. Soc. Lond. A* **1998**, *454*, 903–995. [[CrossRef](#)]
40. Luukko, P.; Helske, J.; Räsänen, E. Introducing libeemd: A program package for performing the ensemble empirical mode decomposition. *Computat. Stat.* **2016**, *31*, 1–13. [[CrossRef](#)]
41. Ministry of Environment Protection of China. *Ambient Air Quality Standards (GB3095–2012)*; China Environmental Science Press: Beijing, China, 2012.
42. World Health Organization. *Air Quality Guidelines—Global Update 2005*; WHO: Geneva, Switzerland, 2006.
43. China MEP Expose 9 Big Cities' Pollution Source, Nanjing Blame Fired-Coal. Available online: http://www.njhb.gov.cn/43123/201504/t20150402_3248553.html (accessed on 30 April 2016).
44. Pastuszka, J.S.; Rogula-Kozłowska, W.; Zajusz-Zubek, E. Characterization of PM₁₀ and PM_{2.5} and associated heavy metals at the crossroads and urban background site in Zabrze, Upper Silesia, Poland, during the smog episodes. *Environ. Monit. Assess.* **2010**, *168*, 613–627. [[CrossRef](#)] [[PubMed](#)]
45. Hu, J.; Wang, Y.; Ying, Q.; Zhang, H. Spatial and temporal variability of PM_{2.5} and PM₁₀ over the North China Plain and the Yangtze River Delta, China. *Atmos. Environ.* **2014**, *95*, 598–609. [[CrossRef](#)]
46. Yang, L.; Gao, X.; Wang, X.; Nie, W.; Wang, J.; Gao, R.; Xu, P.; Shou, Y.; Zhang, Q.; Wang, W. Impacts of firecracker burning on aerosol chemical characteristics and human health risk levels during the Chinese New Year Celebration in Jinan, China. *Sci. Total Environ.* **2014**, *476*, 57–64. [[CrossRef](#)] [[PubMed](#)]
47. Wang, J.; Ogawa, S. Effects of meteorological conditions on PM_{2.5} concentrations in Nagasaki, Japan. *Int. J. Environ. Res. Public Health* **2015**, *12*, 9089–9101. [[CrossRef](#)] [[PubMed](#)]

48. Li, J.J.; Wang, G.H.; Wang, X.M.; Cao, J.J.; Sun, T.; Cheng, C.L.; Meng, J.J.; Hu, T.F.; Liu, S.X. Abundance, composition and source of atmospheric PM_{2.5} at a remote site in the Tibetan Plateau, China. *Tellus B* **2013**, *65*, 20281. [[CrossRef](#)]
49. Charron, A.; Harrison, R.M. Fine (PM_{2.5}) and coarse (PM_{2.5–10}) particulate matter on a heavily trafficked London highway: Sources and processes. *Environ. Sci. Technol.* **2005**, *39*, 7768–7776. [[CrossRef](#)] [[PubMed](#)]



© 2016 by the authors; licensee MDPI, Basel, Switzerland. This article is an open access article distributed under the terms and conditions of the Creative Commons Attribution (CC-BY) license (<http://creativecommons.org/licenses/by/4.0/>).